Preprints of the 19th World Congress
The International Federation of Automatic Control
Cape Town, South Africa. August 24-29, 2014

Dynamic positioning of a diver tracking surface platform

Nikola Mišković, Đula Nađ, Antonio Vasilijević, Zoran Vukić *

* *University of Zagreb, Faculty of Electrical Engineering and Computing, LABUST - Laboratory for Underwater Systems and Technologies, Unska 3, Zagreb, Croatia (e-mail: nikola.miskovic@fer.hr).*

AbstractThis paper presents experimental results obtained on an autonomous omnidirectional surface marine platform, developed at the University of Zagreb, during two-week field trials in Murter, Croatia. We focus on results that are a part of the second phase of research on the platform that is intended to be used as a diver tracking platform. This phase includes experimental verification of the control and dynamic positioning (DP) algorithms performed in real environmental conditions, where external disturbances and sensor characteristics have significant influence on the vehicle behaviour. Specifically, we demonstrate *1)* experimental results showing successful heading control of the overactuated marine platform even in cases when the platform is performing simultaneous omnidirectional motion; *2)* experimental results demonstrating the quality of the DP algorithm performance, and *3)* how GPS update frequency influences the quality of DP performance and the quality of the commanded control signal with the navigation filter that uses only GPS measurement and an uncoupled dynamic model of the omnidirectional marine platform.

Keywords: marine systems; autonomous vehicles; robot navigation; global positioning systems;

1. INTRODUCTION

The research area of marine robotics is becoming more popular as the need to understand the marine environment (underwater and surface) increases both for scientific and economic reasons. There is a substantial number of research groups all over the world who contribute to marine robotics research by developing their own underwater and surface autonomous marine platforms to be used for testing envisioned scenarios and algorithms. Autonomous marine surface vessels are mostly being developed for science (e.g. exploration and observation, environmental data gathering and sampling, Caccia et al. [2007]), bathymetric mapping (e.g. Manley [1997]), defense (e.g. mine-countermeasures Djapic and Nad [2010]), and general robotics research. A concise overview of some developed prototype vessels can be found in Manley [2008].

The Laboratory for Underwater Systems and Technologies (LABUST) at the University of Zagreb, Croatia have developed an overactuated autonomous surface marine platform (shown in Fig. 1) capable of omnidirectional motion while keeping desired heading. The main purpose of this platform is to serve as a diver tracking unit. LABUST has, in cooperation with their partners who are professional divers, demonstrated that cooperation between autonomous marine vehicles and divers is the most appropriate path towards increasing diver safety, enabling diver navigation and monitoring from the surface. A step further in the development of the diver dedicated system is introducing an autonomous underwater vehicle capable of interacting with the diver. This step will be taken within the European FP7 project "CADDY - Cognitive Autonomous Diving Buddy" (611373).

The autonomous surface platform, that carries the international flag marking underwater activity, is overactuated with 4 thrusters forming the "X" configuration. This configuration enables motion in the horizontal plane under any orientation. The current version of the platform is 0.35m high, 0.707m wide and long, as it is shown in Fig. 1, and it weighs approximately 25kg. The control computer (isolated from environmental disturbances inside the platform hull) executes control and guidance tasks (dynamic positioning, path following, diver following) and all the data processing. The complete control architecture is developed in the ROS environment.

The research that involves the use of the described platform has been divided into the following phases:

First phase: Simulations A number of simulation experiments where elementary control and dynamic positioning algorithms were tested under realistic simulation conditions. Additionally, the diver tracking algorithms were included in these simulations where special attention was devoted to ensuring realistic modeling of the sensors used in the platform.

Second phase: Basic experiments This phase includes experimental verification of the control and dynamic

* This work is supported by the Business Innovation Agency of the Republic of Croatia (BICRO) through the Proof of Concept programme, and by European Commission under the FP7–ICT project "CADDY – Cognitive Autonomous Diving Buddy" under Grant Agreement Number: 611373.

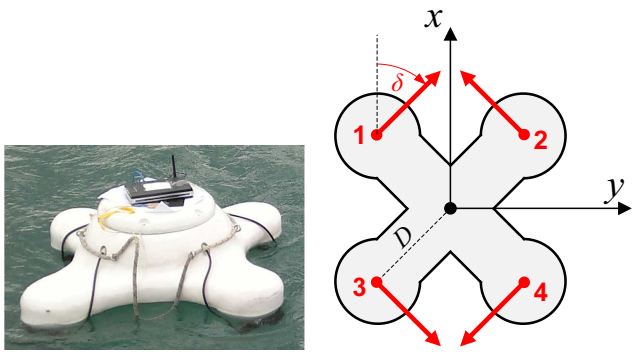

(a) (b)

Figure 1. (a) Prototype of the diver tracking platform developed in LABUST and (b) actuator configuration.

positioning algorithms performed in real life conditions, where external disturbances and sensor characteristics have significant influence to the vehicle behaviour.

Third phase: Diver tracking experiments This phase includes experimental verification of the developed diver tracking algorithms. Quality of the results obtained with divers in the real–life environment is observed.

The simulation phase results have been reported and analyzed in Miskovic et al. [2013] where the proof of concept for diver tracking algorithms has been demonstrated. The experimental results for both the second and the third phase have been obtained in September and October 2013 in Murter, Croatia during a two-week field trial period. This paper reports the experimental results related to the second phase, which involves basic experiments, i.e. control and dynamic positioning algorithms and their quality.

Specifically, this paper will focus on demonstrating the following three topics related to the experimental control and dynamic positioning results obtained on the omnidirectional autonomous surface platform for diver tracking:

(1) experimental results demonstrating successful heading control of the overactuated marine platform even in cases when the platform is performing simultaneous omnidirectional motion;
(2) experimental results demonstrating the quality of the dynamic positioning algorithm performance with the navigation filter that uses only GPS measurement and an uncoupled dynamic model of an overactuated marine platform; and
(3) how GPS update frequency influences *i)* the quality of DP performance and *ii)* the quality of the commanded control signal while using a navigation filter fusing only GPS data with the dynamic model of an overactuated marine platform.

The paper is organized as follows. Section II presents the platform mathematical models while Section III briefly describes the implemented control algorithms. Section IV presents experimental results obtained in a real–life environment and Section V focuses on the analysis of GPS quality relative to the experimental results. The paper is concluded with Section VI.

2. MATHEMATICAL MODELING

Dynamic model Following the notation given in Fossen [1994], dynamic model of the platform in the horizontal plane can be described using the velocity vector $\boldsymbol{\nu} = [\, u \;\; v \;\; r \,]^{\mathrm{T}}$ where u, v and r are surge, sway and yaw speed, respectively; and the vector of actuating forces and moments acting on the platform $\boldsymbol{\tau} = [\, X \;\; Y \;\; N \,]^{\mathrm{T}}$ where X, Y are surge and sway forces and N is yaw moment. Both vectors are defined in the body-fixed (mobile) coordinate frame. The uncoupled dynamic model in the horizontal plane is given with (1) where $\mathbf{M}$ is a diagonal matrix with mass and added mass terms and $\mathbf{D}(\boldsymbol{\nu})$ is a diagonal matrix consisting of nonlinear hydrodynamic damping terms.

$$\mathbf{M}\dot{\boldsymbol{\nu}} = -\mathbf{D}(\boldsymbol{\nu}) + \boldsymbol{\tau} \tag{1}$$

Since the platform is designed to be symmetrical with respect to the x and y axes in the body fixed frame, the following forms of the two matrices are adopted: $\mathbf{M} = diag(\, \alpha_u, \; \alpha_u, \; \alpha_r \,)$, $\mathbf{D}(\boldsymbol{\nu}) = diag(\, \beta_u(u), \; \beta_u(v), \; \beta_r(r) \,)$.

Kinematic model The kinematic translatory equations for the platform motion in the horizontal plane on the sea surface is given with (2), where x and y are the position and ψ is the orientation of the platform in the Earth–fixed coordinate frame and $\mathbf{R}(\psi)$ is the rotation matrix.

$$\begin{bmatrix} \dot{x} \\ \dot{y} \\ \dot{\psi} \end{bmatrix} = \underbrace{\begin{bmatrix} \cos\psi & -\sin\psi & 0 \\ \sin\psi & \cos\psi & 0 \\ 0 & 0 & 1 \end{bmatrix}}_{\mathbf{R}(\psi)} \begin{bmatrix} u \\ v \\ r \end{bmatrix} \tag{2}$$

Additional equation in the kinematic model is $\dot{\psi} = r$. The platform is overactuated, i.e. it can move in any direction in the horizontal plane by modifying the surge and sway speed, while attaining arbitrary orientation.

Actuator allocation The actuator allocation matrix $\boldsymbol{\Phi}$ gives relation between the forces exerted by thrusters $\boldsymbol{\tau}_{\mathbf{i}} = [\, \tau_1 \;\; \tau_2 \;\; \tau_3 \;\; \tau_4 \,]^{\mathrm{T}}$ and the forces and moments $\boldsymbol{\tau}$ acting on the rigid body. Actuator configuration of the autonomous surface platform for diver tracking is given in Fig. 1(b) where $\delta = 45°$. The allocation matrix is given with (3).

$$\boldsymbol{\tau} = \underbrace{\begin{bmatrix} \cos 45° & \cos 45° & -\cos 45° & -\cos 45° \\ \sin 45° & -\sin 45° & \sin 45° & -\sin 45° \\ D & -D & -D & D \end{bmatrix}}_{\boldsymbol{\Phi}} \boldsymbol{\tau}_{\mathbf{i}} \tag{3}$$

3. CONTROL DESIGN

3.1 Speed controller design

For the low–level, speed controller we choose a PI controller in the form

$$\boldsymbol{\tau} = \mathbf{K}_{\mathbf{P}\boldsymbol{\nu}}(\boldsymbol{\nu}^* - \tilde{\boldsymbol{\nu}}) + \mathbf{K}_{\mathbf{I}\boldsymbol{\nu}} \int (\boldsymbol{\nu}^* - \tilde{\boldsymbol{\nu}})\, dt + \boldsymbol{\tau}_{\mathbf{F}} \tag{4}$$

where $\boldsymbol{\nu}^* = [\, u^* \;\; v^* \;\; r^* \,]^{\mathrm{T}}$ are the desired linear and angular speeds of the platform, $\mathbf{K}_{\mathbf{P}\boldsymbol{\nu}} = diag(\, K_{Pu}, \; K_{Pv}, \; K_{Pr} \,)$ and $\mathbf{K}_{\mathbf{I}\boldsymbol{\nu}} = diag(\, K_{Iu}, \; K_{Iv}, \; K_{Ir} \,)$ are diagonal matrices with proportional and integral gains for individual degrees of freedom, respectively. The tilde sign marks the estimated values – the vehicle's speeds are often estimated

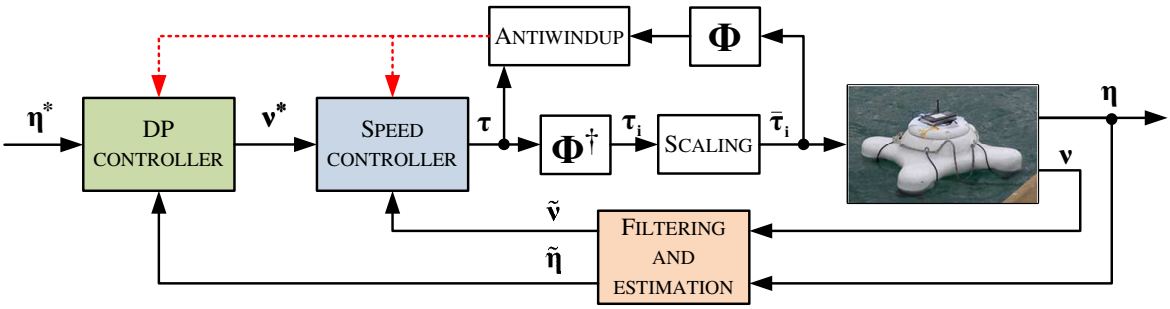

Figure 2. Dynamic positioning and speed control scheme.

since they are either difficult to measure or are unreliable. The $\boldsymbol{\tau}_{\mathbf{F}}$ term represents additional action introduced in the controller to improve the closed loop behaviour, Caccia et al. [2008]. This action can be in the form $\boldsymbol{\tau}_{\mathbf{F}} = \mathbf{D}(\boldsymbol{\nu})\,\boldsymbol{\nu}$ which results in the feedback linearization procedure where measured or estimated speeds are used to compensate for the nonlinearity in the process. Faulty estimation can lead to instability of the closed loop due to the nature of feedback linearization. This is why it is much more convenient to use the reference speed signal instead of the measurements, i.e. $\boldsymbol{\tau}_{\mathbf{F}} = \mathbf{D}(\boldsymbol{\nu}^*)\,\boldsymbol{\nu}^*$ which leads to the feedforward action. It should be mentioned that, theoretically, both the feedback linearization and the feedforward approach result in the same closed loop behaviour. Controller parameters $\mathbf{K}_{\mathbf{P}\boldsymbol{\nu}}$ and $\mathbf{K}_{\mathbf{I}\boldsymbol{\nu}}$ can be calculated based on the desired closed loop characteristic equation as it is shown in Caccia et al. [2008]. These parameters will naturally depend on the parameters of the dynamic model which have to be identified. The dynamic model parameters of the platform that is addressed in this paper have been identified using the identification method based on self–oscillations reported in Miskovic et al. [2011].

3.2 Dynamic positioning (DP) controller design

Since the platform is overactuated, it can move in a horizontal plane while keeping a desired heading. The high–level dynamic positioning controller is of PI type since it compensates all environmental disturbances. In addition to that, the integral action will compensate all the unmodelled dynamics and ensure convergence of the desired position while holding the desired heading ψ^*. The DP controller can be written in the form

$$\boldsymbol{\nu}^* = \mathbf{R}^{\mathrm{T}}(\psi)\left(-\mathbf{K}_{\mathbf{P}\boldsymbol{\eta}}\mathbf{e} - \mathbf{K}_{\mathbf{I}\boldsymbol{\eta}}\int \mathbf{e}dt\right) \tag{5}$$

where $\mathbf{e} = \boldsymbol{\eta}^* - \tilde{\boldsymbol{\eta}}$ is the control difference and $\mathbf{K}_{\mathbf{P}\boldsymbol{\eta}}$ and $\mathbf{K}_{\mathbf{I}\boldsymbol{\eta}}$ are diagonal proportional and integral gain matrices, respectively, chosen so that desired heading closed loop dynamics is achieved. This controller will ensure convergence to the desired position vector $\boldsymbol{\eta}^* = [\,x^*\;\; y^*\;\; \psi^*\,]^T$.

3.3 Filtering, estimation and antiwindup

All the control and guidance algorithms onboard the surface platform are executed at 10 Hz. The Kalman filtering and estimation takes measurements from compass and GPS unit as inputs. Both these measurements can be sampled with a frequency 10 Hz. However, in cases when the sampling frequency is less than 10 Hz, Kalman filtering is implemented in order to estimate the signals in between the measurements. In addition to that, Kalman filter can improve overall system behaviour by fusing GPS measurements with the dynamic model of the platform. In order to keep focus of the paper, details on Kalman filtering and estimation are omitted. For the same reason, the description of the implemented antiwind mechanism is omitted and the interested reader is referred to Miskovic et al. [2013].

4. EXPERIMENTAL RESULTS

The experiments with the platform were performed during two weeks in September and October 2013 on the island of Murter, Croatia. The experiments present results obtained in real environment conditions that have been changing from day to day. For these reasons, a statistical analysis of the relevant experiments is provided.

4.1 Heading control

The following set of experimental results will demonstrate the behaviour of the previously described dual–loop heading control algorithm implemented on the omnidirectional autonomous marine platform in the cases when sway and surge motion are active and inactive.

Surge and sway motions are inactive, demonstrating the pure yaw behaviour of the platform. Fig. 3(a) shows the heading response while the applied surge and sway force were zero. The average overshoot of the system is cca. 10% with the time to reach the maximum overshoot value of about 5 s. Depending on the commanded heading change, the time to reach the steady state will increase due to the saturation of the commanded yaw moment N. The commanded (unsaturated) and achieved (saturated) yaw moment are shown in Fig. 3(a). It is clear that the antiwindup algorithm is working properly since there are no delays in the controller output when the commanded yaw moment is within the saturation bounds.

All three degrees of freedom are active and commanded thrusts and moment are limited to keep them within the feasibility region. The following set of experiments focuses on the scenario when the platform keeps a desired heading while surge and sway forces are applied.

When the platform starts moving in either surge or sway direction, the heading controller is required to generate

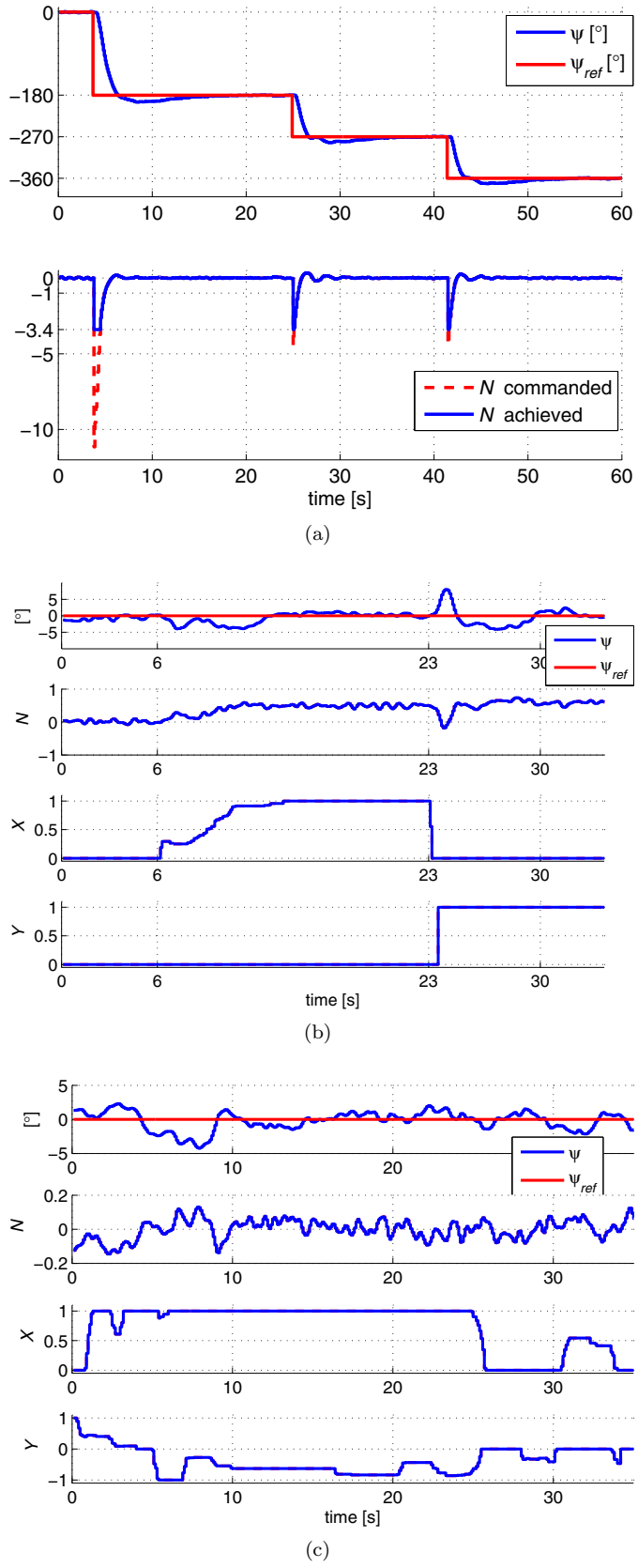

Figure 3. Heading response with surge and sway force (a) inactive, (b) applied consecutively and (c) applied arbitrarily.

additional yaw moment in order to compensate for the disturbances caused by hydrodynamic effects on the platform hull due to the translatory motion. Fig. 3(b) demonstrates this effect when maximal surge and sway forces were applied independently at $t = 6s$ and $t = 23s$, respectively. During the experiment the heading controller managed to keep the heading in the limits $\pm 5°$ at all times except when the abrupt change from surge to sway motion was required at cca $t = 23s$. This is when the coupling effects have the greatest influence.

The most common scenario when constant heading is required while the operator is applying arbitrary surge and sway force simultaneously is shown in Fig. 3(c). The results show that heading behaviour is within $\pm 5°$ regardless of the platform bearing even when coupling effects are the most emphasized.

4.2 Dynamic positioning results

A large number of DP experiments were performed in order to show the consistency in the obtained results. One example of the experiment scenario is shown in Fig. 4(a) where the platform was commanded to dynamically position on four different points. The navigation filter applied in the experiments uses only GPS measurement and an uncoupled dynamic model of the overactuated marine vessel. It should be mentioned that the behaviour of the platform transitioning between two points is pure "line–of–sight" behaviour that is under the strong influence of external disturbances, Chen et al. [2013]. Fig. 4(b) shows the North and East position of the platform (relative to the starting point) together with the absolute value of control errors. These errors are zoomed in to the interesting area around 0 (in the vicinity of the DP points). During this experiment, the DP errors were mostly under 1 m.

5. ANALYSIS OF GPS QUALITY

The GPS unit that was used during the experiments is Locosys LS20031. The quality of the GPS signal significantly depends on the weather conditions. As a consequence, during the days of running field tests, the overall quality of the GPS signal varied, both in precision as well as signal fluctuation. In order to quantify the quality of the signal, we observed DP experiments during 7 days. For each day, set of experiments where the platform was required to perform DP were observed and average GPS measurement distance with respect to the desired coordinates was analyzed. Two measures of quality are defined:

(1) *GPS error* - the average distance of the platform from the commanded DP coordinates, as given by pure GPS measurements only; and
(2) *GPS variation* - the standard deviation of the distance of the platform from the commanded DP coordinates, as given by pure GPS measurements only. This measure indicates the fluctuation of the GPS signal.

As it is shown in Fig. 5, the GPS error, as defined before, varied from around 0.5 m to 2 m. The variation of the signal was generally larger during days with larger GPS error. These results show that, if the quality of the dynamic positioning experiments is to be determined, a statistical

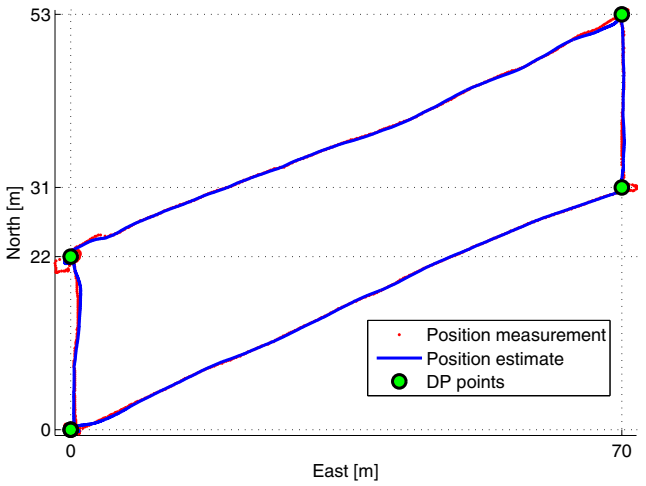

(a)

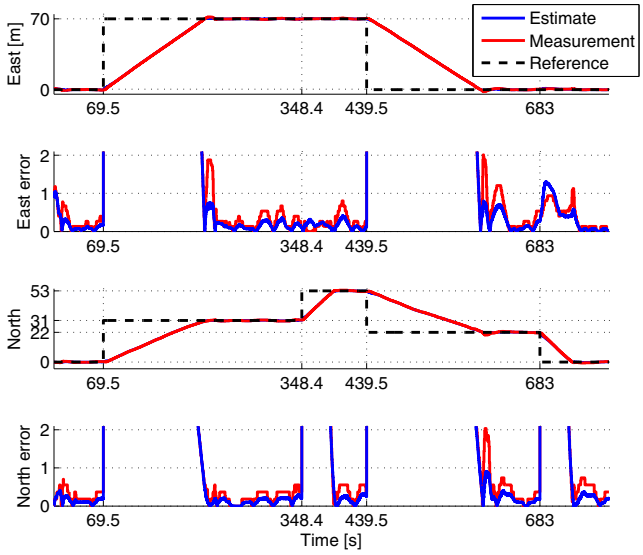

(b)

Figure 4. (a) Position plot and (b) time responses of a scenario where the platform is dynamically positioning around four points.

analysis over results taken during a larger period of time should be performed.

5.1 Influence of GPS update frequency to DP performance

Since the GPS signal can be imprecise, we wanted to test the behaviour of the system with 1 Hz, 2Hz and 10 Hz GPS measurement update rate. The implemented Kalman filter estimates position measurements in order to ensure 10 Hz control execution. We gathered about 170 mins of data at the three update frequencies all together, during the seven days of experiments at different environmental conditions. The quality of the system was compared with respect to two criteria: 1) ratio of errors and variations of the filtered position and unfiltered GPS measurement with respect to the commanded DP point, and 2) average and maximal thruster activity during dynamic positioning.

Criterion 1: Ratio of error and variation of filtered position and unfiltered GPS measurement For each experiment,

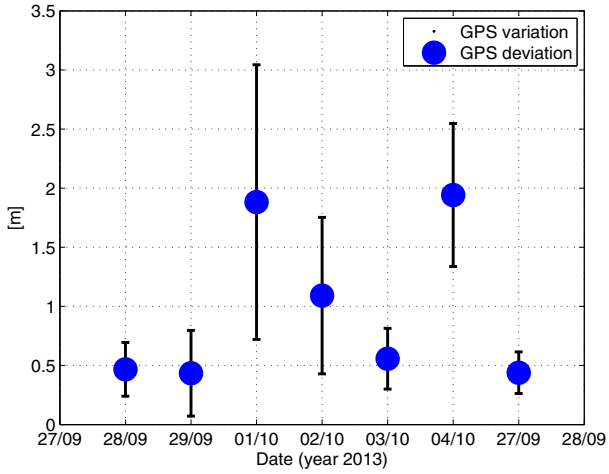

Figure 5. GPS signal quality during DP tests over 7 days of field trials.

measured distance d_{meas} and estimated distance d_{estim} (from the Kalman filter) to the commanded point was observed. For each GPS update frequency we observed measures given with (6) and (7).

$$\text{ratio of errors} = \frac{\text{average}\,(|d_{meas}|)}{\text{average}\,(|d_{estim}|)} \tag{6}$$

$$\text{ratio of variations} = \frac{\text{standard deviation}\ (|d_{meas}|)}{\text{standard deviation}\ (|d_{estim}|)}. \tag{7}$$

The "ratio of errors" shows how many times has the error of the estimated position improved in comparison to the measurement, while "ratio of variations" shows how many times has the variation (fluctuation) of the estimate reduced in comparison to the measured signal. The results are shown in Fig. 6(a). The lower the frequency of GPS measurement update, the behaviour of the position estimate is better (lower error and variation) since the measurements are taken into account less often. According to the obtained results, the estimated position error is about 3 times lower when applying 1 Hz GPS updates, 2 times smaller with 2 Hz updates and 1.5 times smaller with 10 Hz updates.

Criterion 2: Average and maximal thruster activity during DP. For each DP experiment we observed the commanded signal to one thruster and recorder the average absolute value of the derivative of the commanded thrust (jerk) commanded and an average maximal value of the derivative of the commanded thrust in time frames of 1.5 s. These two measures show us the smoothness of the commanded signal, with the requirement that the command signal should be as smooth as possible during DP. Given that the maximal command applied to one thruster is 255, the obtained results are shown in percentage in Fig. 6(b).

The results show that the higher the GPS update frequency, the lower both the average and maximal thruster activity are. While the average activity always remains below 4% of the maximal commanded thrust, the maximal thruster activity in the case of 1 Hz update rate is around 20%. These thruster jumps appear when the GPS measurement arrives (every second) and the Kalman filter needs to correct the estimate.

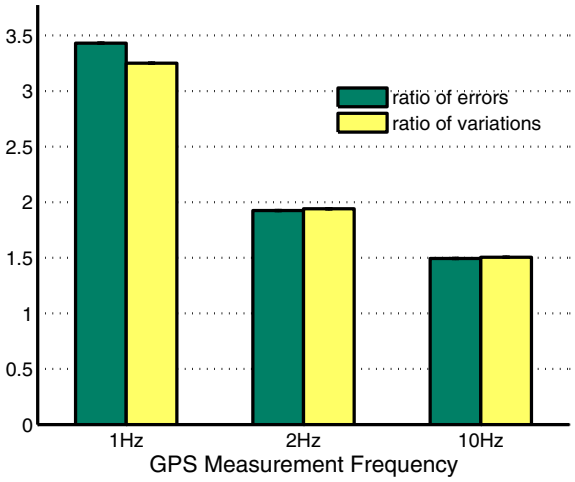

(a)

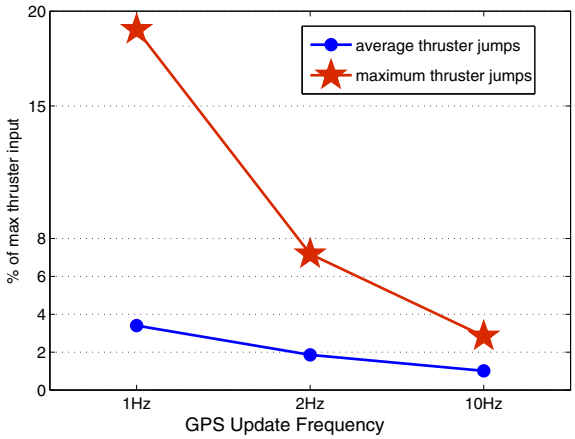

(b)

Figure 6. DP quality assessment in terms of (a) ratio of errors (6) and ratio of variations (7) between measured and estimated positions relative to GPS update frequency, and (b) thruster activity relative to GPS update frequency.

5.2 Comment

The fact that the thruster activity is extreme in the case of 1 Hz update, leads to the conclusion that higher update rates are required, at the expense of higher variation of the position estimate. From the thruster activity perspective, the best choice would be to exploit the maximal GPS update rate. However, in that case, if the environmental conditions are such that GPS measurement fluctuates e.g. $\pm 2m$, the position estimate will fluctuate about 1.5 times less ($\pm 1.3m$) which in some applications may not be acceptable.

The conclusion is that the operator can modify the GPS update rate according to the GPS quality and system performance requirements, in order to achieve the acceptable performance of the system. The main assumption in this analysis is that the estimation filter parameters are set based on the best of knowledge of the system, as was the case in the experiments presented in this paper.

6. CONCLUSIONS

The paper presents experimental verification of control and dynamic positioning algorithms performed in real life conditions during two-week trials on the island of Murter, Croatia. We have demonstrated successful heading control of the overactuated marine platform even in cases when the platform is performing simultaneous omnidirectional motion, the quality of the dynamic positioning algorithm performance with the navigation filter that uses only GPS measurement and an uncoupled dynamic model of an overactuated marine platform, and how GPS update frequency influences the quality of DP performance and the quality of the commanded control signal. The analysis has shown that lower GPS update frequency results in good quality of the position estimate (relative to the GPS measurements) at the expense of high (even unacceptable) thruster activity, while higher GPS update frequency results in smooth thruster activity at the expense of lower quality of the position estimate. Based on the current GPS signal quality, the operator can decide on the required update rate given the presented analysis.

Further work in this field will be devoted to the diver tracking algorithms and demonstration of field trial results.

ACKNOWLEDGEMENTS

The authors would like to thank Nikola Stilinović and Milan Marković for their support during the field trials.

REFERENCES

M. Caccia, M. Bibuli, R. Bono, Ga. Bruzzone, Gi. Bruzzone, and E. Spirandelli. Unmanned Surface Vehicle for coastal and protected water applications: the Charlie project. *Marine Technology Socety Journal*, 41(2):62–71, 2007.

M. Caccia, M. Bibuli, R. Bono, and G. Bruzzone. Basic navigation, guidance and control of an Unmanned Surface Vehicle. *Autonomous Robots*, 25(4):349–365, 2008.

Chen-Wei Chen, Jen-Shiang Kouh, and Jing-Fa Tsai. Modeling and simulation of an auv simulator with guidance system. *Oceanic Engineering, IEEE Journal of*, 38(2):211–225, 2013.

V. Djapic and D. Nad. Using collaborative autonomous vehicles in mine countermeasures. In *OCEANS 2010 IEEE - Sydney*, pages 1–7, 2010.

T.I. Fossen. *Guidance and Control of Ocean Vehicles*. John Wiley & Sons, New York, NY, USA, 1994.

J.E. Manley. Development of the autonomous surface craft "ACES". In *Proc. of Oceans'97*, volume 2, pages 827–832, 1997.

J.E. Manley. Unmanned Surface Vehicles, 15 years of development. In *Proc. of MTS/IEEE Oceans'08*, Quebec City, Canada, September 2008.

N. Miskovic, Z. Vukic, M. Bibuli, G. Bruzzone, and M. Caccia. Fast in-field identification of unmanned marine vehicles. *Journal of Field Robotics*, 28(1):101–120, 2011. doi: 10.1002/rob.20374.

N. Miskovic, E. Nad, N. Stilinovic, and Z. Vukic. Guidance and control of an overactuated autonomous surface platform for diver tracking. In *Control Automation (MED), 2013 21st Mediterranean Conference on*, pages 1280–1285, 2013. doi: 10.1109/MED.2013.6608884.